Acta Crystallographica Section F
Structural Biology and Crystallization Communications
ISSN 1744-3091

Crystallization and preliminary X-ray analysis of enoyl-acyl carrier protein reductase (FabK) from *Streptococcus pneumoniae*

Jun Saito,* Mototsugu Yamada, Takashi Watanabe, Hideo Kitagawa and Yasuo Takeuchi

Pharmaceutical Research Center, Meiji Seika Kaisha Ltd, 760 Morooka-cho, Kohoku-ku, Yokohama 222-8567, Japan

Correspondence e-mail: jun_saito@meiji.co.jp

Received 7 March 2006
Accepted 9 May 2006

The enoyl-acyl carrier protein (ACP) reductase from *Streptococcus pneumoniae* (FabK; EC 1.3.1.9) is responsible for catalyzing the final step in each elongation cycle of fatty-acid biosynthesis. Selenomethionine-substituted FabK was purified and crystallized by the hanging-drop vapour-diffusion method at 277 K. The crystal belongs to space group $P2_1$, with unit-cell parameters $a = 50.26$, $b = 126.70$, $c = 53.63$ Å, $\beta = 112.46^\circ$. Diffraction data were collected to 2.00 Å resolution using synchrotron beamline BL32B2 at SPring-8. Two molecules were estimated to be present in the asymmetric unit, with a solvent content of 45.1%.

1. Introduction

The bacterial type II fatty-acid synthase complex comprises discrete enzyme activities encoded by discrete genes, in contrast to the multifunctional type I fatty-acid synthase in mammals (Rock & Cronan, 1996; Cronan & Rock, 1996). Therefore, these bacterial enzymes are attractive targets for the development of novel selective antibacterial agents (Heath *et al.*, 2001). Enoyl-acyl carrier protein (ACP) reductase (EC 1.3.1.9) is responsible for catalyzing the final step in each elongation cycle of bacterial type II fatty-acid biosynthesis and plays a key role in the regulation of the pathway (Heath & Rock, 1995, 1996). Indeed, enoyl-ACP reductase activity is required for maintaining cell viability, as demonstrated from analyzing a *fabI* (Ts) mutant in *Escherichia coli* (Heath & Rock, 1995) and by using FabI-specific inhibitors. Triclosan is known to inhibit FabI, the enoyl-ACP reductase from *E. coli* (Heath *et al.*, 1998) and *Staphylococcus aureus* (Heath *et al.*, 2000; Slater-Radosti *et al.*, 2001). The anti-tuberculosis agent isoniazid also targets the FabI homologue (InhA) of *Mycobacterium tuberculosis* (Quémard *et al.*, 1995).

Recent genomic studies have demonstrated that an alternative triclosan-resistant enoyl-ACP reductase, FabK, is present in several clinical pathogens (Heath & Rock, 2000). For example, FabK is the sole enoyl-ACP reductase in *Streptococcus pneumoniae* and both FabI and FabK have been found in pathogens such as *Enterococcus faecalis* and *Pseudomonas aeruginosa* (Heath & Rock, 2000). Although novel FabI inhibitors targeting *Staph. aureus* have been reported by several groups (Heerding *et al.*, 2001; Ling *et al.*, 2004; Seefeld *et al.*, 2001), there are very few reports of FabK-specific inhibitors, except for a small number of compounds with weak inhibitory activity (Seefeld *et al.*, 2003; Payne *et al.*, 2002). Therefore, an inhibitor designed to selectively target FabK is anticipated to have a narrow spectrum of antimicrobial activity against *Strep. pneumoniae*, including penicillin-resistant *Strep. pneumoniae* (PRSP). However, an inhibitor targeting both FabI and FabK should have a broader spectrum of activity against *Staph. aureus*, including methicillin-resistant *Staph. aureus* (MRSA), *Enterococci*, including *E. faecalis* and vancomycin-resistant *Enterococci* (VRE), and *P. aeruginosa*, including the multiple drug-resistant *P. aeruginosa* (MDRP).

Crystal structures of FabI from several sources have been determined (Pidugu *et al.*, 2004), but the structure of FabK is still not available. In order to facilitate the development of selective FabK and/or dual FabK/FabI inhibitors by structure-based drug design, we have initiated a three-dimensional structure analysis of FabK from

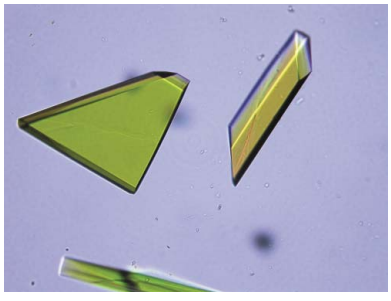

Table 1
Diffraction data statistics of SeMet-substituted FabK.

Values in parentheses are for the highest shell.

	Remote	Peak	Edge
X-ray source	SPring-8, BL32B2		
Detector	Jupiter 210 CCD detector		
Temperature (K)	100		
Space group	$P2_1$		
Unit-cell parameters			
a (Å)	50.26		
b (Å)	126.70		
c (Å)	53.63		
β (°)	112.46		
Wavelength (Å)	0.90000	0.97888	0.97932
Resolution range (Å)	39.00–2.00 (2.07–2.00)	39.00–2.00 (2.07–2.00)	39.00–2.00 (2.07–2.00)
Total reflections	140565 (14285)	139889 (14041)	148999 (15001)
Unique reflections	78798 (7763)	79294 (7812)	79789 (7909)
$R_{\rm merge}$	0.086 (0.199)	0.064 (0.139)	0.062 (0.142)
Completeness (%)	95.4 (94.0)	96.1 (94.9)	97.2 (96.2)
Mean $I/\sigma(I)$	3.9 (1.8)	6.6 (3.1)	7.6 (3.5)
$\Delta f'$		−6.63	−8.22
$\Delta f''$		5.37	3.71

Strep. pneumoniae. In this paper, we describe the crystallization and preliminary X-ray analysis of this enzyme.

2. Expression and purification

The FabK gene from *Strep. pneumoniae* R6 (GenBank accession No. AE008418) was amplified by PCR using 5′-GGAATTCCATATGAAAACGCGTATTACAGAA-3′ as the forward primer and 5′-CCGCTCGAGGTCATTTCTTACAACTCCTGT-3′ as the reverse primer. The forward and reverse primers included an *Nde*I and *Xho*I restriction recognition site, respectively. The amplified PCR fragment was digested with *Nde*I and *Xho*I and then ligated into the pET-21b(+) expression vector (Novagen, Madison, WI, USA) at the corresponding sites. The resulting construct encoded full-length FabK (residues 1–324) with a C-terminal tag containing Leu-Glu followed by a His_6 purification tag. Nucleotide sequencing of the insert was performed to ensure that no mistakes had been introduced during the amplification process. The final construct was then transformed into the *E. coli* methionine auxotroph B834 (DE3) (Novagen).

The cells were cultivated in 5 l LeMaster medium (LeMaster & Richards, 1985) containing SeMet supplemented with 50 µg ml^{-1} ampicillin at 310 K to an OD_{600} of 0.6. IPTG was added to a final concentration of 1 m*M* and growth was continued for an additional 3 h. The cells were harvested by centrifugation and resuspended in buffer *A* [50 m*M* sodium phosphate pH 8.0, 300 m*M* NaCl, 1 m*M* phenylmethylsulfonyl fluoride (PMSF), 1 m*M* benzamidine and 1 m*M* β-mercaptoethanol] containing 5 m*M* imidazole and 0.1 mg ml^{-1} lysozyme. The mixture was incubated for 30 min at ice temperature and then sonicated on ice. The cell lysates were centrifuged at 27 000*g* for 30 min in order to remove cell debris. The supernatant was filtered with a 0.22 µm filter and loaded onto a column packed with 30 ml Ni–NTA Agarose beads (Qiagen, Valencia, CA, USA) equilibrated with buffer *A* containing 5 m*M* imidazole. The column was washed with buffer *A* containing 20 m*M* imidazole and bound protein was eluted with buffer *A* containing 200 m*M* imidazole. Fractions containing FabK were identified by SDS–PAGE and subsequently pooled and dialyzed against buffer *B* [50 m*M* Tris–HCl pH 7.5, 50 m*M* NH_4Cl, 1 m*M* PMSF, 1 m*M* benzamidine and 1 m*M* dithiothreitol (DTT)]. The dialysate was loaded onto a POROS HQ/20 column (PerSeptive Biosystems, Framingham, MA, USA) equilibrated with buffer *B*. The column was washed with buffer *B* and bound proteins were eluted with a linear gradient of 0–500 m*M* NaCl in buffer *B*. Fractions containing FabK were identified by SDS–PAGE and subsequently pooled. Ammonium sulfate was added to the pooled fractions to a final concentration of 2.0 *M* and the mixture was applied onto a Resource PHE 6 ml column (Amersham Biosciences, Uppsala, Sweden) equilibrated with buffer *B* containing 2.0 *M* ammonium sulfate. After the column had been washed with buffer *B* containing 2.0 *M* ammonium sulfate, the protein was eluted with a decreasing linear gradient of 2.0–0 *M* ammonium sulfate in buffer *B*. Fractions containing FabK were identified by SDS–PAGE and subsequently concentrated by ultrafiltration using an Amicon Ultra-15 centrifugal filter device with a 30K NMWL (Millipore, Bedford, MA, USA). The concentrated sample was loaded onto a HiLoad 16/60 Superdex 75 prep-grade size-exclusion column (Amersham Biosciences) equilibrated with buffer *B* containing 150 m*M* NaCl. The peak fractions were pooled and then concentrated to 10 mg ml^{-1} and the buffer exchanged to 10 m*M* Tris–HCl pH 7.5, 100 m*M* NH_4Cl, 5 m*M* DTT and 5 m*M* NADH by ultrafiltration as described earlier.

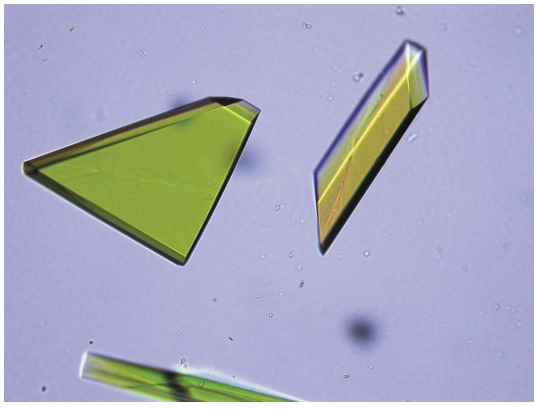

Figure 1
Crystals of SeMet-substituted FabK.

3. Crystallization

SeMet-substituted FabK crystals were grown by the hanging-drop vapour-diffusion method at 277 K. Initial screening was performed using sparse-matrix screens (Jancarik & Kim, 1991) based on the commercially available Crystal Screens I and II (Hampton Research, Laguna Niguel, CA, USA) and Wizard I and II (Emerald Biostructures, Bainbridge Island, WA, USA) and additional crystallography reagent kits. Several crystal forms were obtained and the most promising crystallization condition was optimized. 2 µl protein solution (10 mg ml^{-1}) was mixed with an equal volume of reservoir solution and equilibrated against 0.5 ml reservoir solution at 277 K. Microcrystals were obtained with reservoir solution containing 0.1 *M* MES pH 5.5–7.0, 0.1 *M* NH_4Cl, 0.2 *M* $CaCl_2$, 8–15%(*v*/*v*) MPD, 8–15%(*w*/*v*) PEG 1000 and 5 m*M* DTT. Several microcrystals were washed with reservoir solution and then crushed to produce microseeds, which were stored in 10 µl reservoir solution. For microseeding experiments, the seed stock was diluted 10^4-fold to 10^6-fold with the reservoir solution. A 2 µl aliquot of this prepared precipitant was mixed with 2 µl protein solution to make the droplet. Finally, thin plate-shaped crystals of SeMet-substituted FabK were obtained with average dimensions of approximately 0.05 × 0.30 × 0.50 mm (Fig. 1).

4. Data collection

A crystal of SeMet-substituted FabK was transferred to a reservoir solution with 15%(*w*/*v*) glycerol as a cryoprotectant for several seconds and flash-cooled in a cryostream of N_2 gas at 100 K. A multiple-wavelength anomalous dispersion (MAD) data set was collected on the pharmaceutical industry beamline (BL32B2) at the SPring-8 synchrotron facility (Hyogo, Japan) using a Jupiter 210 CCD detector (Rigaku, Tokyo, Japan). The values of $\Delta f'$ and $\Delta f''$ were determined experimentally with X-ray absorption fine-structure (XAFS) spectroscopy after the mounting the crystal on the beamline. The oscillation ranges were 220° and three wavelengths were used in the sequence high-energy remote (0.90000 Å), peak (0.97888 Å) and edge (0.97932 Å), with the oscillation per frame being 1° in each case. All X-ray diffraction data were integrated and scaled using the *CrystalClear* package (Rigaku). Diffraction data statistics are summarized in Table 1. The space group of the SeMet-substituted FabK crystal was determined to be monoclinic $P2_1$. Assuming the presence of two molecules of FabK in the asymmetric unit, the value of the Matthews coefficient V_M is 2.24 Å^3 Da^{-1}, corresponding to a solvent content of 45.1%, both of which are within the normal range of values for protein crystals (Matthews, 1968). The search for Se-atom sites and the structure determination of FabK using the MAD method is now in progress.

We thank Dr Y. Katsuya for help with XAFS spectroscopy and data collection. We also thank K. Nagano for technical assistance with protein expression and purification.

References

Cronan, J. E. Jr & Rock, C. O. (1996). *Escherichia coli and Salmonella typhimurium: Cellular and Molecular Biology*, 2nd ed., edited by F. C. Neidhardt, R. Curtis, J. L. Ingraham, E. C. C. Lin, K. B. Low, B. Magasanik, W. Reznikoff, M. Riley, M. Schaechter & H. E. Umbarger, pp. 612–636. Washington DC: American Society for Microbiology.
Heath, R. J., Li, J., Roland, G. E. & Rock, C. O. (2000). *J. Biol. Chem.* **275**, 4654–4659.
Heath, R. J. & Rock, C. O. (1995). *J. Biol. Chem.* **270**, 26538–26542.
Heath, R. J. & Rock, C. O. (1996). *J. Biol. Chem.* **271**, 1833–1836.
Heath, R. J. & Rock, C. O. (2000). *Nature (London)*, **406**, 145–146.
Heath, R. J., White, S. W. & Rock, C. O. (2001). *Prog. Lipid Res.* **40**, 467–497.
Heath, R. J., Yu, Y. T., Shapiro, M. A., Olson, E. & Rock, C. O. (1998). *J. Biol. Chem.* **273**, 30316–30320.
Heerding, D. A., Chan, G., DeWalf, W. E. Jr, Fosberry, A. P., Janson, C. A., Jaworski, D. D., McManus, E., Miller, W. H., Moore, T. D., Payne, D. J., Qiu, X., Rittenhouse, S. F., Slater-Radosti, C., Smith, W., Tanaka, D. T., Vaidya, K. S., Yuan, C. C. K. & Huffman, W. F. (2001). *Biorg. Med. Chem. Lett.* **11**, 2061–2065.
Jancarik, J. & Kim, S.-H. (1991). *J. Appl. Cryst.* **24**, 409–411.
LeMaster, D. M. & Richards, F. M. (1985). *Biochemistry*, **24**, 7263–7268.
Ling, L. L., Xian, J., Ali, S., Geng, B., Fan, J., Mills, D. M., Arvantes, A. C., Orgueira, H., Ashwell, M. A., Carmel, G., Xiang, Y. & Moir, D. T. (2004). *Antimicrob. Agents Chemother.* **48**, 1541–1547.
Matthews, B. W. (1968). *J. Mol. Biol.* **33**, 491–497.
Payne, D. J. *et al.* (2002). *Antimicrob. Agents Chemother.* **46**, 3118–3124.
Pidugu, L. S., Kapoor, M., Surolia, N., Surolia, A. & Suguna, K. (2004). *J. Mol. Biol.* **343**, 147–155.
Quémard, A., Sacchettini, J. C., Dessen, A., Vilcheze, C., Bittman, R., Jacobs, W. R. Jr & Blanchard, J. S. (1995). *Biochemistry*, **34**, 8235–8241.
Rock, C. O. & Cronan, J. E. Jr (1996). *Biochem. Biophys. Acta*, **1302**, 1–16.
Seefeld, M. A. *et al.* (2003). *J. Med. Chem.* **46**, 1627–1635.
Seefeld, M. A., Miller, W. H., Newlander, K. A., Burgess, W. J., Payne, D. J., Rittenhouse, S. F., Moore, T. D., DeWolf, W. E. Jr, Keller, P. M., Qiu, X., Janson, C. A., Vaidya, K., Fosberry, A. P., Smyth, M. G., Jaworski, D. D., Slater-Radosti, C. & Huffman, W. F. (2001). *Biorg. Med. Chem. Lett.* **11**, 2241–2244.
Slater-Radosti, C., Van Aller, G., Greenwood, R., Nicholas, R., Keller, P. M., DeWolf, W. E. Jr, Fan, F., Payne, D. J. & Jaworski, D. D. (2001). *J. Antimicrob. Chemother.* **48**, 1–6.